Molecular Model of the Interaction of Bee Venom Phospholipase A_2 with Manoalide

Angel R. Ortiz,† M. Teresa Pisabarro,† Federico Gago*

Departamento de Fisiología y Farmacología, Universidad de Alcalá de Henares, 28871 Madrid, Spain

Received January 21, 1993

A molecular model of the interaction between manoalide (MLD) and bee venom phospholipase A_2 (bv-PLA_2) has been derived making use of a combination of computational methods. MLD was built in its open form and simulated by using molecular dynamics techniques. It is shown that the polar part of the molecule, which is thought to be the reactive region, is endowed with considerable conformational flexibility whereas the apolar region is rather rigid. The proposed active conformation of MLD and the main putative binding site for MLD on this enzyme were identified by matching potential energy GRID maps for both ligand and receptor with the chemical structure of the respective counterpart. The binding site is found in the C-terminal region of bv-PLA_2, forming part of the proposed interfacial surface for binding to aggregated substrates, and comprises two distinct regions: (i) a hydrophobic cavity delimited by the C-terminal β-sheet and the antiparallel β-sheet, which interacts with the apolar zone of MLD, and (ii) a cationic site made up of residues Arg-58 and Lys-94, which interacts with the polar zone. Molecular dynamics and molecular orbital calculations indicate that the most likely initial reaction between MLD and bv-PLA_2 is formation of a Schiff base between Lys-94 and the aldehyde generated upon opening of MLD's γ-lactone ring, supporting recent model reaction studies. The inhibition seems to be a consequence of the occupation by MLD of a site overlapping a phosphocholine binding site in bv-PLA_2 presumably involved in the interface desolvation process. The present model represents a starting point for further structural studies on the mechanism of phospholipases A_2 inactivation by MLD and MLD-like compounds.

Introduction

Manoalide (MLD), a sesterterpenoid (Figure 1a) isolated from the sponge *Luffariella variabilis*,[1] has been shown to be a potent antiinflammatory agent, and in this activity phospholipase A_2 (PLA_2) inhibition is believed to play a major role.[2] In fact, MLD is a potent inhibitor of PLA_2s from several sources,[3] but bee venom PLA_2 (bv-PLA_2) has been shown to be particularly sensitive to inactivation by this molecule.[4] Because of the important role of PLA_2 in the release of arachidonic acid, the biosynthetic precursor of proinflammatory eicosanoids, understanding the molecular mechanism of action of this compound is of considerable interest and can be of help in the design of novel PLA_2 inhibitors.[5]

Although some of the conditions necessary for MLD reactivity have been elucidated, the precise mechanism by which MLD irreversibly inactivates PLA_2s remains largely unknown. Furthermore, even though bv-PLA_2 inhibition is accompanied by the modification of only three, and mainly one,[6] of the 11 lysine residues present in the enzyme, the exact location of the MLD binding site has not been identified as yet. Studies with a structural analogue of MLD called manoalogue have shown that this compound has no affinity for the catalytic site and that manoalogue-modified enzymes still contain a functional active site.[7] On the other hand, whereas a 1:1 stoichiometry of manoalogue to lysine has been demonstrated in cobra venom PLA_2,[8] studies based on the reactivity of MLD with several lysine-containing peptides suggest that a peptide sequence in the enzyme containing a 1,4-Lys arrangement might be involved.[6b]

MLD contains two reactive ring structures, a hemiacetal ring and a γ-lactone ring, which become open at high pH to generate two α,β-unsaturated aldehydes[2b,6,9] (Figure 1b), and an apolar chain that might be involved in hydrophobic interactions with the enzyme.[10] Previous studies have demonstrated that both the opening of the lactone ring and the presence of the free aldehyde groups are required for irreversible inhibition.[7a,9,10] Only very recently have model reactions proved that the initial reaction between MLD and bv-PLA_2 involves the formation of a Schiff base, presumably with a lysine residue.[11]

All of the above-mentioned studies suggest the following sequence of events: (i) unmasking of two α,β-unsaturated aldehydes upon opening of both rings in the MLD molecule and (ii) subsequent binding to a specific site on bv-PLA_2 separate from the active site. Yet the precise binding site and the actual mechanism of bv-PLA_2 inhibition by MLD remain unclear. On the other hand, the reported crystallographic structure of bv-PLA_2 complexed with a transition-state analogue in the active site solved at 2.0-Å resolution[12] has provided us with the foundation for a theoretical analysis of this reaction. In this paper, we use a combination of computational methods to present a molecular model of the interaction between this enzyme and the open form of MLD which accounts for most of the experimental results at the molecular level.[13]

Results

Rationale for Modeling the Open Form of Manoalide. Inhibition studies have indicated that hydrocarbon derivatives containing just the 4-hydroxy-2-butenolide ring of MLD are inhibitory, although in this case the loss of enzyme activity is reversible.[9] On the other hand, methylation of the 4-hydroxy group of MLD's butenolide ring yields compounds that are no longer irreversible PLA_2 inactivators.[7a] These results suggest that the pharmacologically relevant form of MLD is the open form and that the two aldehydes present in this form are required for

* Author to whom correspondence should be addressed.
† Present address: European Molecular Biology Laboratory, Meyerhofstrasse 1, Postfach 10.2209, D-6.900 Heidelberg, Germany.

0022-2623/93/1836-1866$04.00/0

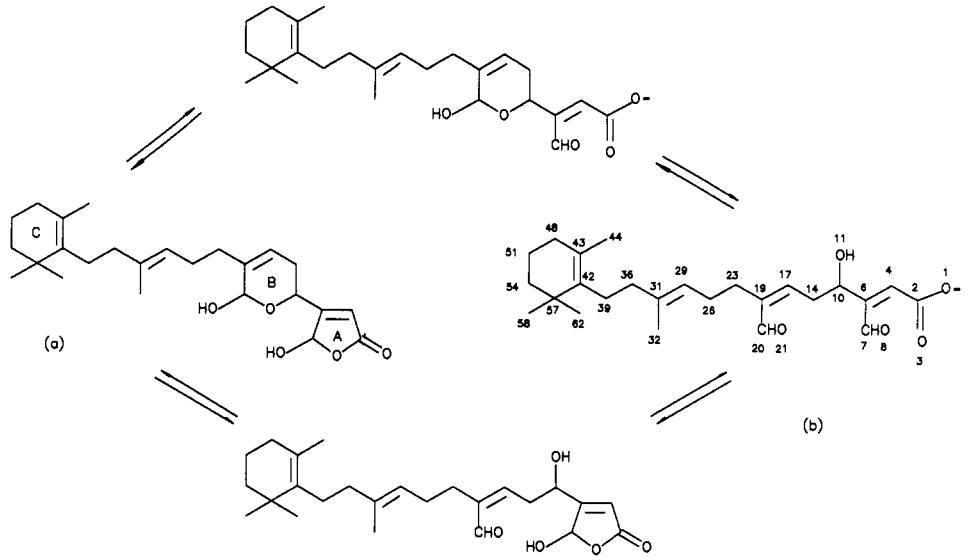

Figure 1. Structure of manoalide in its closed (a) and open form (b).

irreversible addition to PLA_2s. Thus, although both the open and the closed forms of MLD are present in solution, the opening of rings A and B must occur prior to the addition reaction. This implies that the open form must be docked in the binding site of the enzyme immediately before addition takes place. It is reasonable to suppose that this transient state has a half-life at least of the order of picoseconds, which is the time scale of our molecular dynamics simulations. Therefore our modeling of the noncovalent complex only involves the study of the step most proximate to the initiation of the addition reaction and does not take into account the interaction of the closed form of MLD with the enzyme, if it takes place at all. It is also reasonable to suppose that this short-life complex must be stable, or otherwise the probability of attack would be very low. This means that the open form of MLD must interact favorably with the enzyme and must stay in the binding site in a low-energy conformation.

Conformational Search for Putative Active Conformations of MLD. The high-temperature molecular dynamics method was chosen in our search for the putative active conformation of MLD because of its efficiency in crossing energy barriers in the multidimensional conformational space.[14] The temperature of 1000 K allows the molecule to explore a number of configurations that are separated by barriers which would be crossed very infrequently at room temperature. This calculation provides us with a sample of conformations and their potential energies. We then assume that the putative active conformation can be found in the lower energy subset of this sample. Thus the probability of finding one or more active conformations is heavily dependent on the conformational space explored. In order to assess the effectiveness of the search, we analyzed three different spaces: the cartesian space, the torsion angle space, and the potential energy space.

1. **Cartesian Space.** Every element in the displacement autocorrelation matrix (DAM) with a root-mean-square deviation of less than 3 Å (an arbitrarily chosen threshold value) is represented as an open square in Figure 2a. Conformational families can thus be identified along the dynamics trajectory based on structural similarity: seven families, numbered from I to VII, can be discerned, each with an average lifetime of about 6–8 ps. However, not all of the conformations within the lifetime of a family belong to the family; that is, small barriers of energy exist between different minima around the conformational family valley, which are crossed in the time scale of 1 ps. Relatively long simulation times separate some families from others, which is suggestive of higher energy barriers between them. In fact, the energy plot (Figure 2b) indicates that a barrier of 5–7 kcal mol^{-1} is separating family II from family III, family III from family IV, and family VI from family VII. On the other hand, the different families have a comparable energy, of about 26 ± 2 kcal mol^{-1}. All in all, these results are indicative, as expected, of a rather complex potential energy surface. Examination of the minimum values for the displacement autocorrelation function (DAF) (Figure 2c) shows that the minimum root-mean-square differences between any pair of conformations separated by a short time are always comparable and that no conformations are revisited during the simulation, which means that the simulation was not run long enough for a thorough search of the phase space. The maximum values for the DAF show a plateau at a root-mean-square value of about 7.5 Å, suggesting that all the conformational space accessible at 1000 K is within a 7.5-Å conformational hypersphere.[14] The small fluctuations in the average values of the DAF are indicating that the molecule did not get trapped in a potential energy well along the simulation, which is in accord with the DAM cluster graph since the squares are distributed in a homogeneous fashion.

2. **Torsion Angle Space.** The total number of conformational hypercubes found was 10 (Table I), a figure comparable to the number of families identified in the previous analysis. It is clear from Table I that not all torsion angles can rotate with the same freedom. The rigidity of the opened γ-lactone together with the possibility of hydrogen-bond formation with the hydroxyl group severely limit the range of conformations available to torsion angles τ_1 and τ_2. Something similar happens to torsion angles τ_8 and τ_9, in this case because of the bulky trimethylcyclohexenyl system. Therefore, most of the conformational flexibility of MLD stems from rotation about torsionals τ_3, τ_4, τ_5, τ_6, and τ_7 (see Table I for definition of these angles).

3. **Potential Energy Space.** One of the risks inherent to high-temperature molecular dynamics simulations is that the structures can get trapped in high-energy local

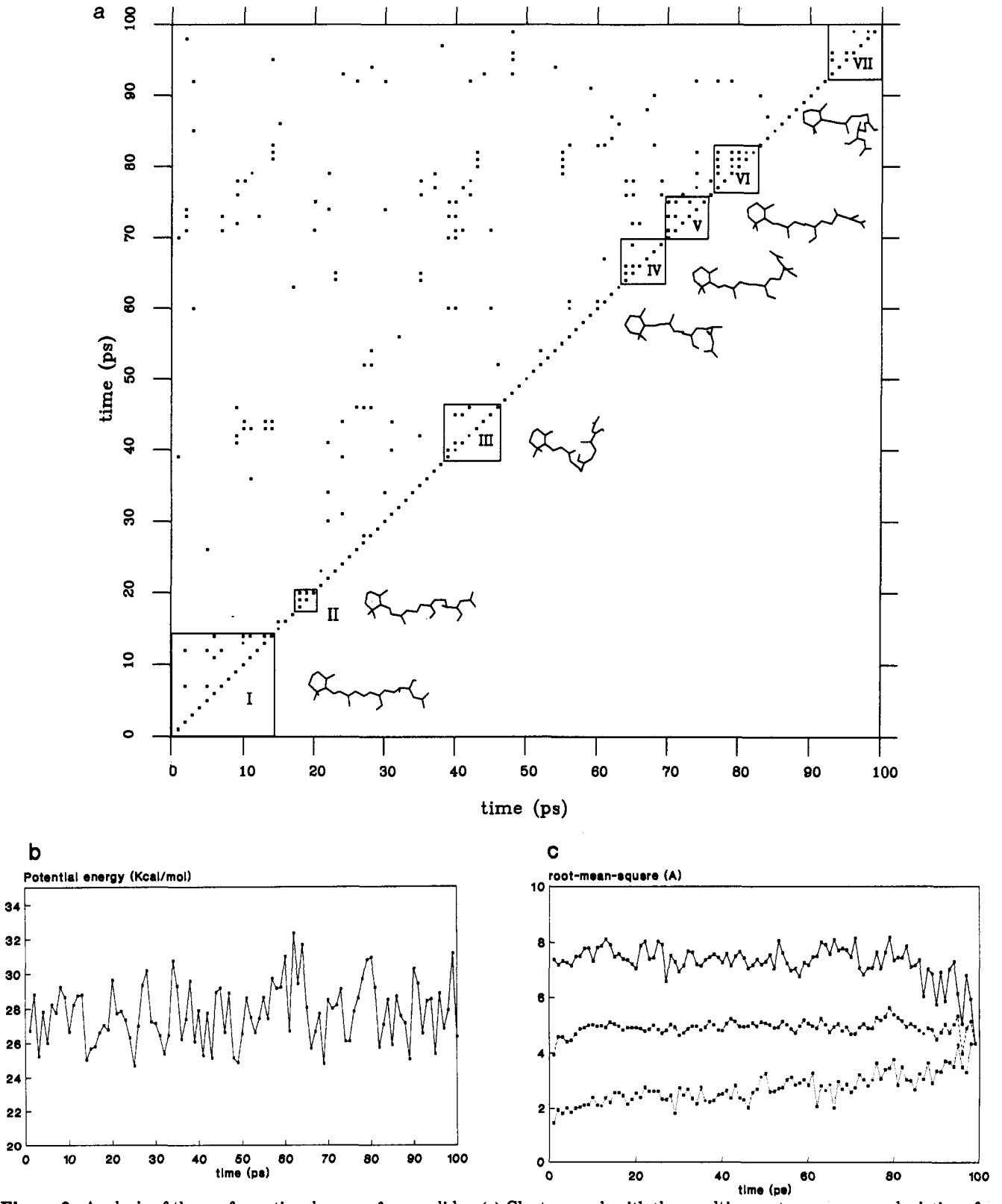

Figure 2. Analysis of the conformational space of manoalide. (a) Cluster graph with the resulting root-mean-square deviations for each pair of structures. The conformer indices are plotted on the x and y axes while the root-mean-square deviations are plotted on the z axis. Only the upper half of the symmetrical displacement autocorrelation matrix is shown. Beside the box around each family of conformers the shape of a representative member is depicted. (b) Potential energy of the 100 minimized structures selected from the 1000 K simulation. (c) Displacement autocorrelation function: average (--□--), minimum (·□·), and maximum (—□—) values.

minima. To avoid this, and in order to complete the search procedure, additional molecular dynamics at 300 K on a representative set of conformers has been deemed necessary.[15] Thirty structures were therefore selected for this last part of the conformational search protocol (Chart I). Figure 3 shows the distribution of conformers as a function of their potential energy values after minimization of the structures obtained from the simulations at 1000 and 300 K. In the 1000 K simulation the distribution follows a bell-shaped, Gaussian-like pattern, again suggestive of the molecule not having been trapped in potential energy valleys, whereas in the 300 K simulation clusters of

Chart I. Quenched Molecular Dynamics Protocol Followed in the Conformational Search for MLD

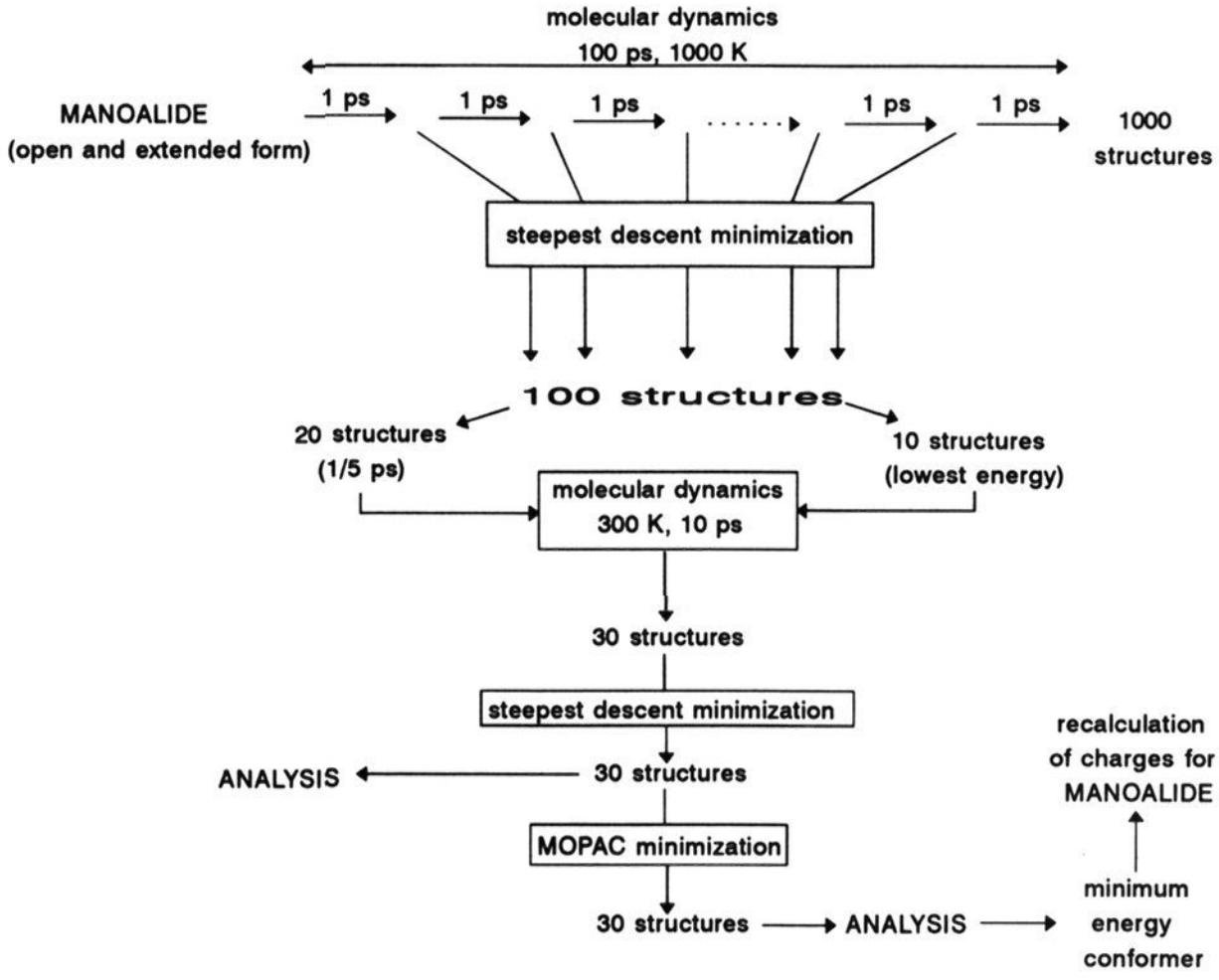

Table I. Number of Hypercubes Found Along the Dynamics Trajectory at 1000 K[a]

hypercube number	τ_1	τ_2	τ_3	τ_4	τ_5	τ_6	τ_7	τ_8	τ_9
1	−	0	+	−	0	+	−	0	+
2	−	−	0	0	0	0	−	0	+
3	−	−	0	+	0	−	0	0	+
4	−	0	0	+	−	0	+	0	+
5	−	0	+	+	−	0	+	0	+
6	+	0	+	0	0	+	0	0	+
7	−	0	+	+	0	0	+	0	+
8	−	0	+	+	+	+	+	0	+
9	−	0	+	−	−	0	−	−	+
10	−	0	−	−	−	0	−	0	+

[a] The torsion angles are defined as: τ_1 = C4–C6–C10–C14, τ_2 = C6–C10–C14–C17, τ_3 = C10–C14–C17–C19, τ_4 = C17–C19–C23–C26, τ_5 = C19–C23–C26–C29, τ_6 = C23–C26–C29–C31, τ_7 = C29–C31–C36–C39, τ_8 = C31–C36–C39–C42, τ_9 = C36–C39–C42–C43.

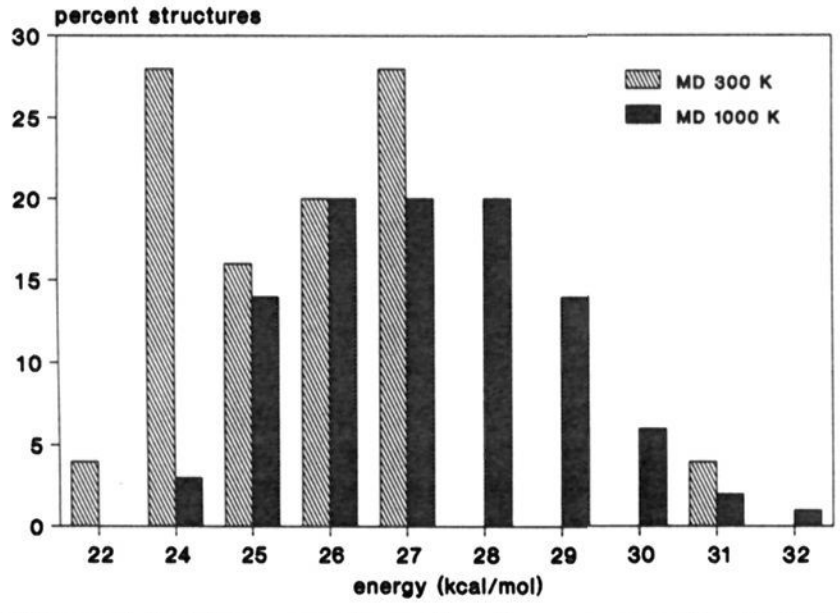

Figure 3. Relative percentage of conformers, according to their potential energy values, found during the dynamics simulations at 300 and 1000 K.

conformers around different energy values are apparent, indicating that the molecule at this temperature did not have enough kinetic energy to overcome the higher energy barriers. It is also evident from this figure that the energy of the structures from the simulation at 300 K is shifted toward lower values, which confirms the view that the dynamics run at 300 K is necessary when searching for low-energy conformations.

Table II. Pseudodihedral Angle (Φ) and Potential Energy (kcal mol^{-1}) of the Nine Most Stable MLD Conformers Found after the Conformational Search both by Molecular Mechanics (MM), Using $\epsilon = 4r_{ij}$, and Molecular Orbital Calculations (H_f, Heat of Formation)[a]

structure number	simulation	MM	H_f	Φ
100	300 K	22.65	−244.70	−60
30	300 K	24.28	−240.67	+60
50	300 K	24.45	−242.46	180
40	300 K	24.48	−244.62	180
25	1000 K	24.66	−242.40	180
69	1000 K	24.76	−245.65	−60
49	1000 K	24.84	−243.72	180
15	300 K	24.90	−240.96	+60
65	300 K	24.97	−245.16	+60
average			−245.51	+60

[a] See text for details.

Location and Description of the Main Putative MLD Binding Site. Of the 130 minimized structures, 12 of them, corresponding to those conformers with a potential energy lower than 25 kcal mol^{-1}, were selected as putative active conformations: 9 were extracted from the 300 K simulation, whereas only 3 came from the 1000 K simulation, again highlighting the importance of the last part of the conformational search procedure. These structures appear superimposed in Figure 4, and their potential energies can be found in Table II. MLD displays several nearly isoenergetic conformations. A pseudodihedral angle connecting the carboxyl group with the trimethylcyclohexenyl moiety can be defined which falls into one of three possible ranges in the mimimum-energy conformations: gauche$^+$ (∼+60°), gauche$^-$ (∼−60°), or trans (∼180°). Assuming that the apolar chain may fit into a hydrophobic pocket[10] and that the carboxyl group may interact with

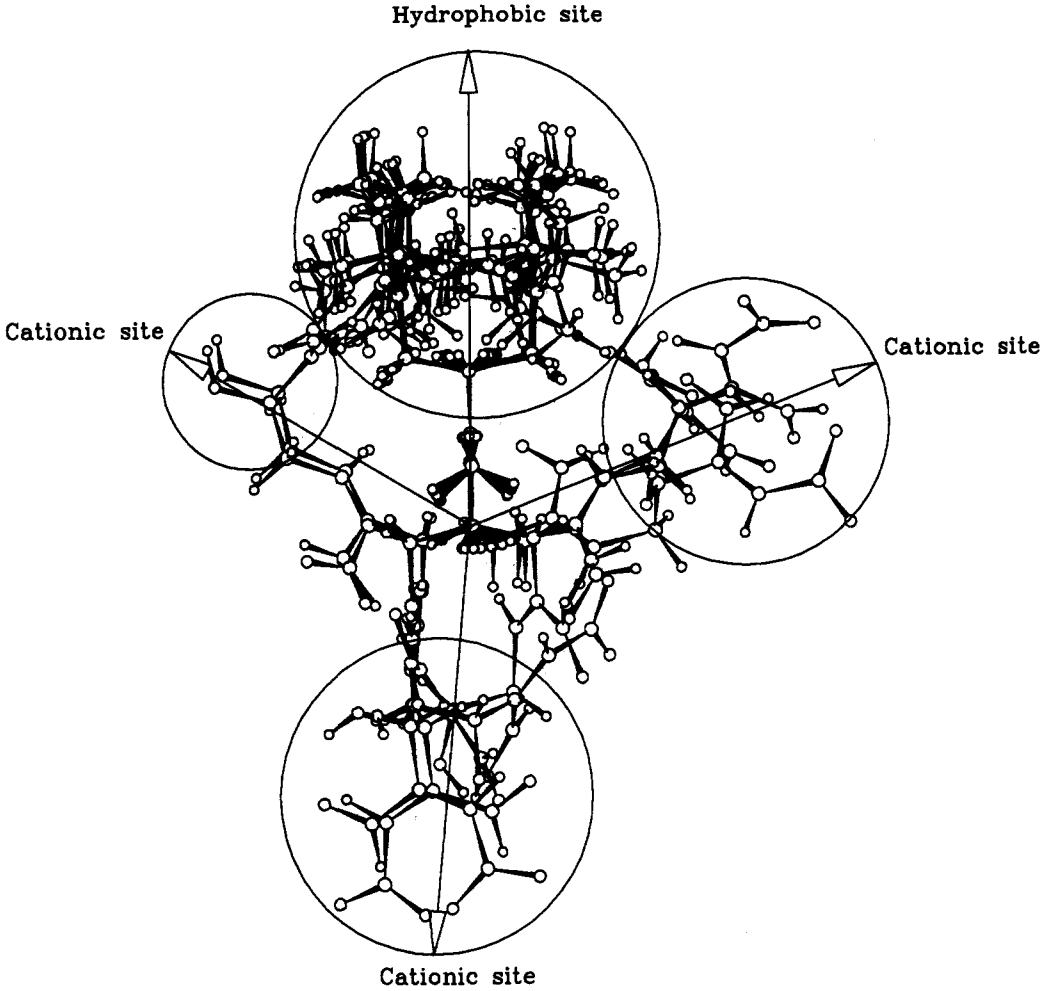

Figure 4. Superimposition of 12 manoalide structures with an energy lower than 25 kcal mol^{-1}. Note the three alternative locations of the plausible cationic site with respect to the putative hydrophobic pocket.

a positively charged region in the receptor, this disposition delineates only three plausible arrangements of chemical groups in the MLD binding site of bv-PLA_2 (Figure 4) and simplifies the process of searching for complementary regions.

In order to locate possible mutually complementary zones in the ligand and in the receptor, each of the nine selected conformers and bv-PLA_2 were probed with several representative chemical groups as described in the Methodology section. We presupposed that if the probes were carefully chosen, it should be possible to find a rough match between the GRID[16] maps around the binding site in the receptor and the chemical structure of the ligand in its putative active conformation and, simultaneously, between the GRID maps around MLD in this conformation and a suitable disposition of chemical groups in the enzyme. Additional prerequisites for this search were (i) that a pocket should be present large enough to fit the ligand, (ii) that a lysine residue be present in the vicinity of the binding site, and (iii) that MLD should fit into this site without any steric clashes.

Two sites on the surface of the enzyme were preselected as potential binding sites. The first site, named *site a*, is made up by residues Cys-105, Cys-113, Trp-128, Phe-129, Tyr-116, Val-102, Pro-101, Arg-58, and Lys-94 and is defined by the interplay between the β-hairpin, the C-terminal β-strand, and the third helix of the enzyme (residues 76–90). This site is located near the so-called *interfacial binding surface*[23] of bv-PLA_2, responsible for the interfacial activation of the enzyme, and also near the hydrophobic channel that interacts with the acyl chains of the natural substrate and leads to the active site. The second site localized, named *site b*, is made up by residues Lys-97, Cys-61, Cys-95, Leu-114, Phe-129, and Tyr-116 and is flanked by Lys-120 and Lys-124. Site b originates from the packing together of the β-hairpin with the second helix of bv-PLA_2 (residues 61–73) and the terminal β-strand. It is thus located opposite to site a and also opposite to the interfacial binding surface.

The active site was also included as a potential binding site for the open form of MLD and named *site c*. Even though it is known from experiment that MLD does not interact with the active site,[2b,6,7] this site contains an important hydrophobic portion and it is large enough to fit the MLD molecule. Therefore site c was included as a *negative control* for the docking studies.

The GRID program was then used to explore these three sites as described in the Methodology section. By manually docking the nine MLD conformers described above, $3 \times 9 = 27$ complexes were generated, and the relative binding energy for MLD in each of them (Figure 5) was calculated as described in Methodology. The calculated binding energies at site c appear to be overestimated in comparison with those at the other two sites. This is partly a consequence of neglecting desolvation of the calcium ion in the binding process and also reflects the fact that the calculated interaction between Ca^{2+} and MLD is not completely reliable because of the inadequacy of using a

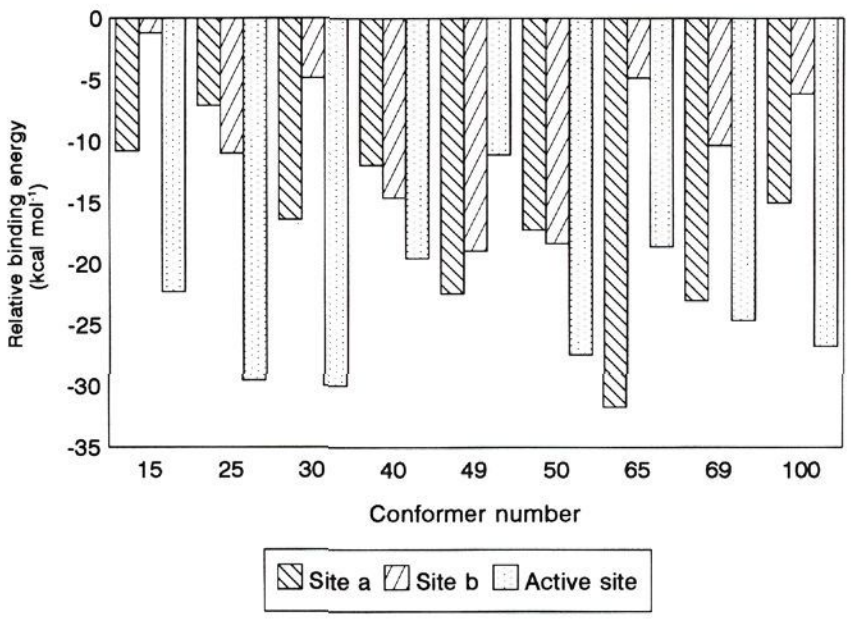

Figure 5. Relative binding energies (kcal mol^{-1}) for MLD in the different complexes studied.

charge of +2 for calcium when *ab initio* calculations[17] show that in the calcium binding site the charge of the calcium ion is about +1. In any case, the most negative binding energy is found between conformer 65 (pseudodihedral angle +60°, Table II) and site a of bv-PLA_2, which we propose as the putative major binding site for MLD. Figure 6 displays the respective GRID maps and the chemical structures of both the open form of MLD and the amino acid residues making up this site. Part of the hydrocarbon backbone of MLD fits very nicely into a green contour representing the favorable interaction of the enzyme with a methyl probe in that region. Likewise, a rough match can be detected between the aliphatic part of Lys-94 and Asp-130 side chains and the yellow contours representing the favorable interaction of the drug in that conformation with a methyl probe. The complementary GRID maps corresponding to the interactions of a negative charge with the enzyme (in red) and a positive charge with the drug (in blue) are also in the right region, although the fit is not so apparent in the figure due to the fact that only the lower energy levels are shown for clarity. Besides, it must be born in mind that the GRID maps were calculated for a particular conformation and one must allow at least for some minor adjustments upon complex formation.

This putative binding site for the open form of MLD is made up of a hydrophobic pocket located between the β-sheet corresponding to residues 127–130 and the antiparallel β-sheet (residues 101–105 and 113–116), along with a positively charged site consisting of Lys-94 and Arg-58. As we mentioned before, this binding site is found on the surface of the enzyme away from the active site (Figure 7), as the experimental data suggest.[2b,6,7] Figure 8 shows MLD docked into this pocket after minimizing the average conformation of the 80–100-ps part of the trajectory. Interestingly, Lys-94 is forming part of this site. This lysine residue is equivalent to Lys-88 in the study of Glaser et al.,[6] the one residue mainly modified by MLD. Therefore, a clear correspondence exists between the 81–128 fragment, pinpointed as the major MLD binding fragment in bv-PLA_2,[6] and the binding site we now describe.

Decomposition of the binding energy between MLD and the enzyme provides a deeper understanding of the principal interactions involved in this complex (Table III). A general agreement with the energy GRID maps discussed above is manifest: the trimethylcyclohexenyl system of MLD interacts with the β-sheets of the enzyme mainly through van der Waals interactions, whereas strong electrostatic attraction is observed between the carboxyl group of MLD and Arg-58 and, secondarily, Lys-94. It could be argued that the shielding effect of the solvent

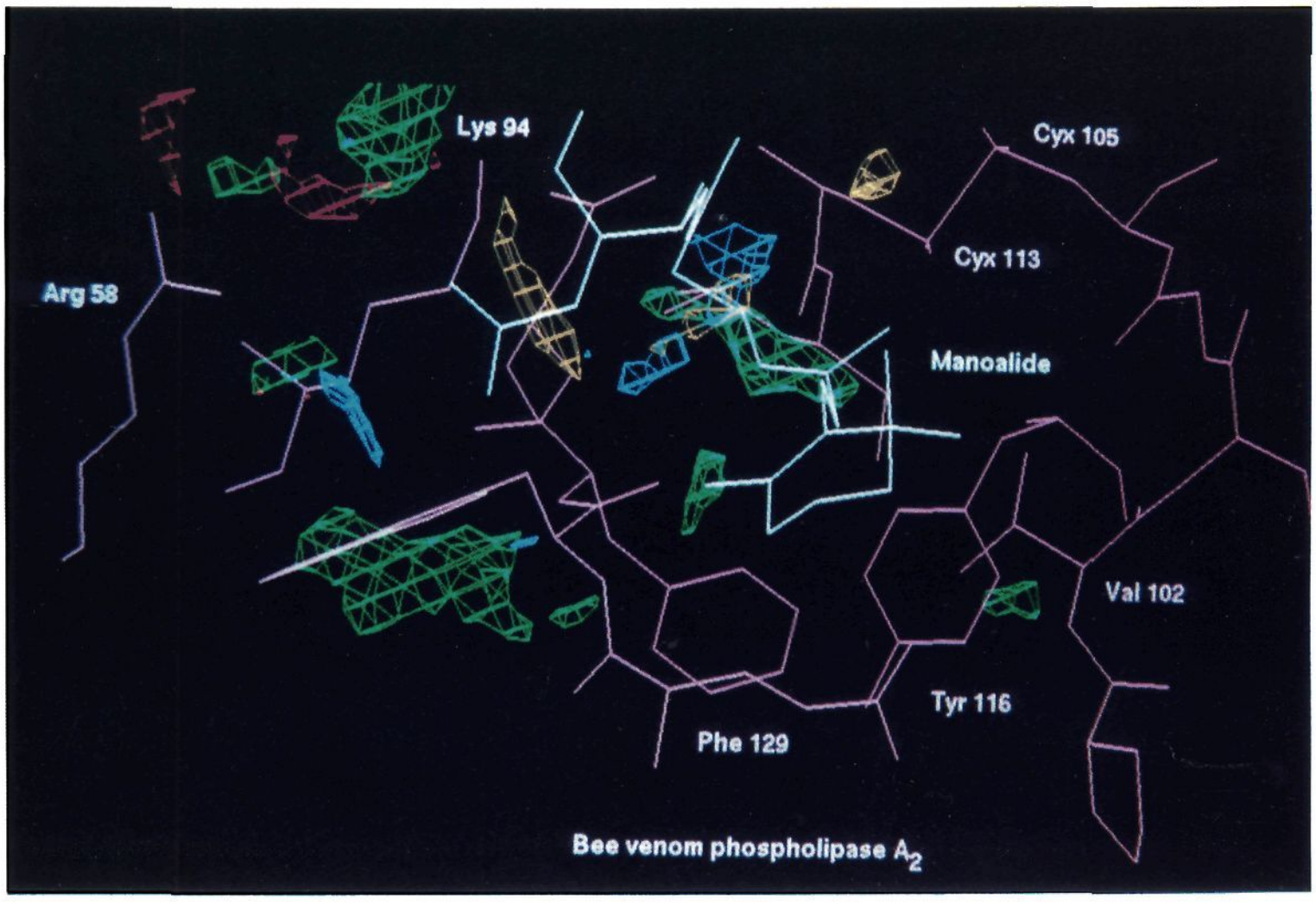

Figure 6. GRID energy maps obtained with methyl (green: −4.0 kcal mol^{-1} contour) and multiatom carboxyl (red: −16.0 kcal mol^{-1} contour) probes on the bv-PLA_2 molecule, and methyl (yellow: −4.0 kcal mol^{-1} contour) and charged sp^3 amino (blue: −12.0 kcal mol^{-1} contour) probes on MLD. Bonds are drawn in white for MLD and in pink for the enzyme. Significant residues for properly orientating the molecule and relevant to the text have been labeled.

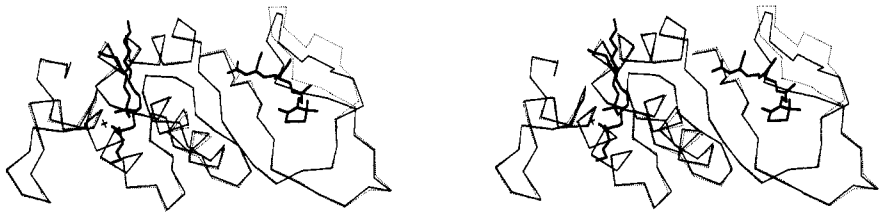

Figure 7. Stereo Cα trace of the X-ray structure of bv-PLA_2 (dotted lines) complexed with L-1-O-octyl-2-heptylphosphonyl-*sn*-glycero-3-phosphoethanolamine in the active site[12] and the MLD–bv-PLA_2 complex described in this paper (solid lines). The calcium ion in the active site is represented as a cross. The transition state analogue appears on the left and manoalide lies on the right hand side (both in thick lines).

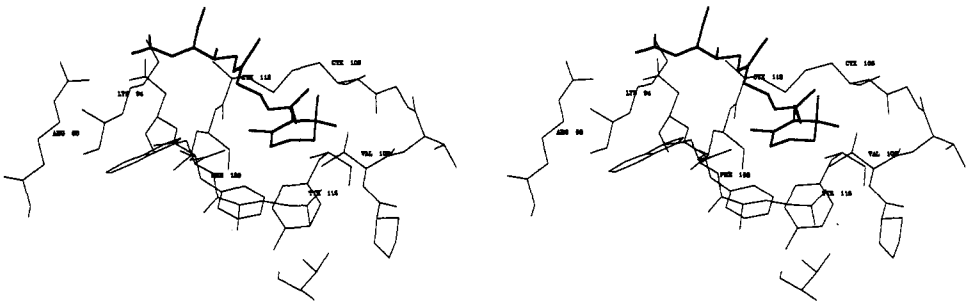

Figure 8. Stereo drawing of MLD (thick lines) docked into the putative binding site of bv-PLA_2. Note both the proximity between lysine-94 and the α,β-unsaturated aldehyde in MLD and the vicinity of arginine-58 to MLD carboxyl group. Residues 101–105, 113–116, and 127–130 are lining the hydrophobic pocket where the trimethylcyclohexenyl head lies.

Table III. Breakdown of the Total Interaction Energy (kcal mol^{-1}) between MLD and bv-PLA_2 (MLD–bv-PLA_2)[a]

residues	region	MLD–bv-PLA_2	NB	ELE	HB
101–105	β-sheet	−3.0	−2.7	−0.3	0.0
113–116	β-sheet	−2.0	−1.9	−0.1	0.0
127–130	β-sheet	−3.4	−8.4	5.0	0.0
125	Val-125	−0.2	−0.2	0.0	0.0
94	Lys-94	−35.9	−1.0	−34.7	−0.2
58	Arg-58	−23.8	−0.7	−22.8	−0.3
solvent		−114.2	−11.8	−98.1	−4.3
rest of the protein		2.0	−2.7	4.7	0.0

[a] ELE is the electrostatic contribution, NB corresponds to the 6–12 nonbonded dispersion–repulsion term, and HB is the corresponding 10–12 term for hydrogen bonding interactions.[36]

should strongly decrease the intensity of these interactions because of the location of both residues on the surface of the macromolecule. The magnitude of this effect can be estimated by computing the solvent surface accessibility of the charged atoms in both residues. This calculation, using the algorithm by Lee and Richards[18] and a probe with a radius of 1.4 Å as implemented in the ACCESS program, shows that the guanidinium group of Arg-58 is partially buried (percent accessibility: NH1 = 34.5, NH2 = 33.3), whereas the ammonium group of Lys-94 is mainly exposed to the solvent (percent accessibility: CE = 99.3, NZ = 56.4), indeed suggesting that electrostatic interactions play an important role in the binding of MLD to the enzyme. Consequently, stronger electrostatic interactions are to be expected between MLD and Arg-58 than between MLD and Lys-94, in agreement with the GRID maps. It has been proposed that hydrophobic interactions are important in the mechanism of bv-PLA_2 inhibition by MLD.[10] The magnitude of these hydrophobic interactions in our modeled complex can be approximated by using the method of Eisenberg and McLachlan,[19] which gives an estimate of −5.5 kcal mol^{-1} for the contribution of hydrophobic forces to the binding free energy, a relatively large value provided mainly by the apolar region of MLD.

The MLD–bv-PLA_2 complex appears to be quite stable during the simulation. MLD deviates slightly from the initial structure (root-mean-square deviation of 0.99 Å for all atoms) so as to enhance its interaction with Arg-58 and Lys-94. On the other hand, the major change in bv-PLA_2, with respect to the crystallographic structure, affects the antiparallel β-sheet (root-mean-square deviation = 1.2 Å), which moves as a rigid body toward MLD in order to maintain closer contacts in the hydrophobic pocket (Figure 7). This motion appears to be coupled to a rotation of the side chain of Asp-130, whose χ_1 torsion angle changes from −64.7 in the crystal structure to −153.2 in the final complex and whose hydrogen bond to the amide of Arg-113 is lost. In turn this rotation is in part originated by an unfavorable interaction energy in the initial complex between this residue and MLD, which is also negatively charged. In order to test whether these collective motions were dependent on inaccuracies in the conditions of the simulation or were in effect originated as a consequence of the ligand–receptor interaction, a 100-ps molecular dynamics simulation was run on bv-PLA_2 alone under the same conditions used for the MLD–bv-PLA_2 complex. Upon averaging out the last 20 ps of the trajectory and quenching by energy minimization, the resulting structure compared very well with the crystallographic one: Asp-130 and the antiparalell β-sheet remained very close to their crystallographic positions. Therefore the collective motions described above appear to be a consequence of the interaction of MLD with bv-PLA_2.

Model for the Reaction Mechanism. Since ring opening in MLD generates two α,β-unsaturated aldehydes and an α,β-unsaturated carboxylic acid, several mechanisms, either singly or in combination, by which a lysine residue could react with MLD are possible: (i) imine formation at the aldehyde groups, (ii) Michael addition at the β position of the α,β-unsaturated aldehydes or carboxylic acid, and (iii) amide formation. A recent interesting model study[11] with MLD methyl analogue and *n*-butylamine in place of the lysine residue has demonstrated that it is the hemiacetal group on the γ-hydroxybutenolide ring which is involved in the reaction and leads to formation of a Schiff base (imine) which can be reversed by treatment with hydroxylamine. Likewise,

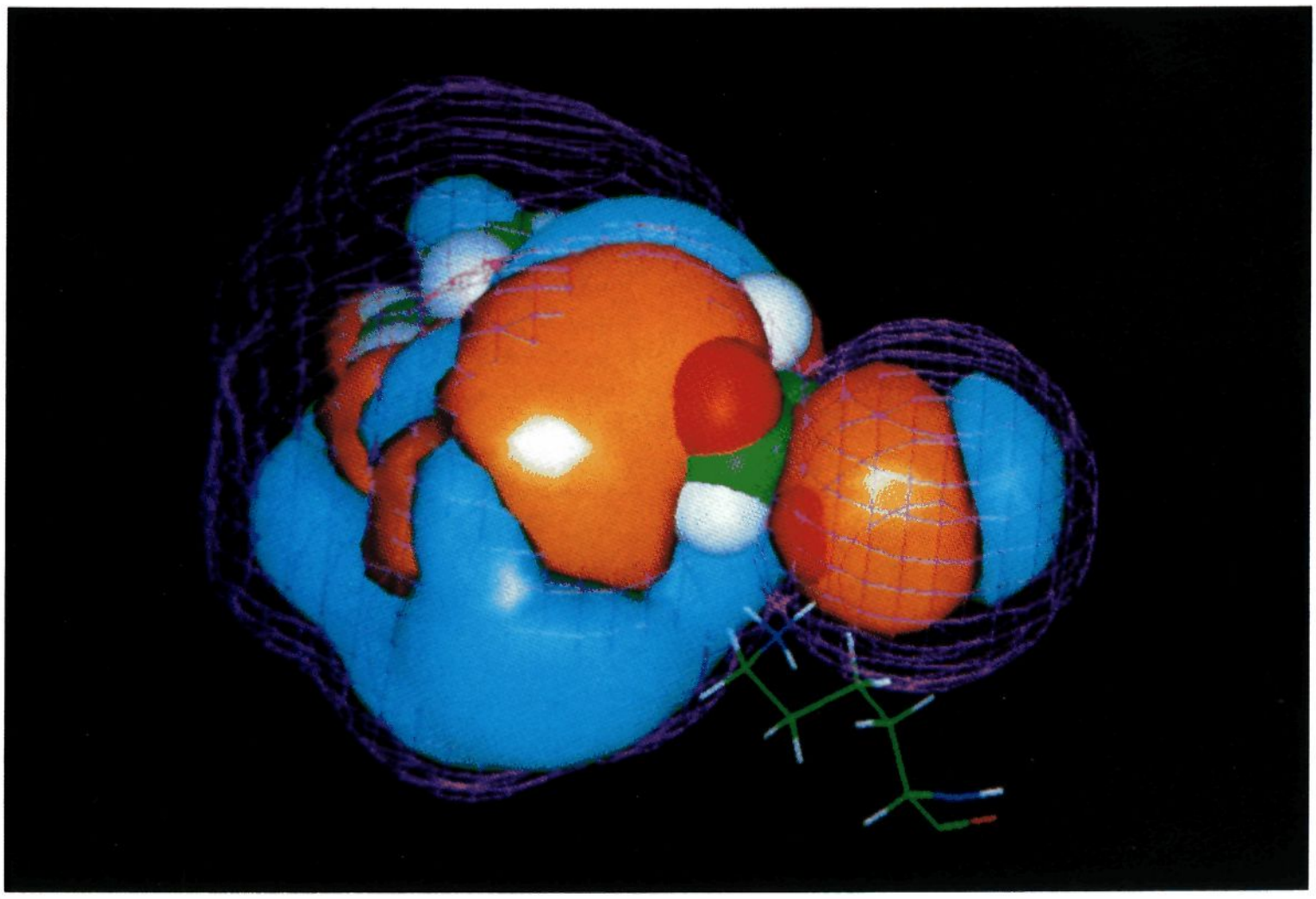

Figure 9. Representation of MLD (space-filling) and Lys-94 (stick) in the MLD–bv-PLA_2 complex. The electron density grid for MLD (magenta) is contoured at 0.0004 electrons/Å^3. The LUMO + (light blue) and LUMO − (orange) for MLD, both contoured at 0.02 (electrons/Å^3)$^{1/2}$, are displayed as opaque solids. The carbonyl C-7 atom (green) appears as the most likely site for nucleophilic attack by this lysine residue.

treatment of the MLD–bv-PLA_2 adduct with hydroxylamine results in substantial recovery of the PLA_2 activity, thereby demonstrating that the initial reaction between MLD and bv-PLA_2 is imine formation presumably involving the aldehyde generated upon opening of ring A and a lysine residue.

In our modeled complex we have addressed this issue by carrying out a molecular orbital calculation on MLD in its putative active conformation. Addition of a nucleophile to MLD will occur preferentially to that part of the molecule in which the lowest unoccupied molecular orbital (LUMO) is the more exposed relative to the total electron density.[20] Figure 9 shows the LUMO of MLD superimposed onto an isovaluated electron density grid together with the properly oriented Lys-94. It can be seen that in its complex with bv-PLA_2 the preferred position in MLD for nucleophilic attack is the carbonyl C-7 atom (C25 in ref 11) and also that the spatial disposition of Lys-94 in the complex nicely suggests that this is the residue likely to perform the attack. The distance between the two reactive centers is also critically important to nucleophilic reactivity.[21] The alignment of MLD in this binding pocket, primarily dominated by the electrostatic and hydrophobic forces described above, enforces a geometric disposition for C-7 that makes it a suitable target for nucleophilic attack. The N–C-7 distance is 4.1 Å in the complex whereas the lysine nitrogen and the alternative carbonyl C-20 atom are 6.3 Å apart. Therefore it is the protein structure which is determining residency of the reactive center of the ligand at a critical distance from its own reactive center. The optimal distance for a reaction of this type is roughly estimated to be 2.8 Å,[21] which implies that both the nucleophile and the electrophile must desolvate prior to forming the reactive complex. As a matter of fact, in our model system a water molecule is roughly equidistant between C-7 of MLD and Nζ of Lys-94 and must leave this site in order for the nucleophilic attack to proceed, thus allowing the two reactive centers to reach a distance closer to 2.8 Å. Taking these arguments together we propose that the initial reaction between MLD and the binding site we describe in bv-PLA_2 is imine formation at C-7 of MLD involving the amino group of Lys-94.

It is obvious that our calculations provide an indication of what the general trend of the reaction could be rather than absolute data but this hypothesis is testable and could lead to further experiments. In any case, the agreement with the results from the model studies is encouraging.

Discussion

The conformational behavior of the open form of MLD has been studied by molecular dynamics techniques. The simulation was too short for the purpose of sampling the whole conformational space but sufficiently long for highlighting the main features of the lower energy conformers, the energy barriers between them and the differential rotational freedom around the different bonds. In particular, it was found that the apolar moiety of MLD is rather rigid, whereas the polar region can visit very separate regions of the surrounding space due to rotations about torsionals τ_4 to τ_6 and the length of the molecule. The minimum-energy conformers fall into three distinct geometrical classes, but since the energy barriers separating them are relatively low it can be thought that the reactive groups of MLD can interact with different arrangements of reactant groups in the enzyme. All that is needed is a large hydrophobic pocket and a vicinal positively charged region. In other words, MLD is rather unspecific because it can adapt its molecular structure to different environments. This behavior can help to explain why MLD

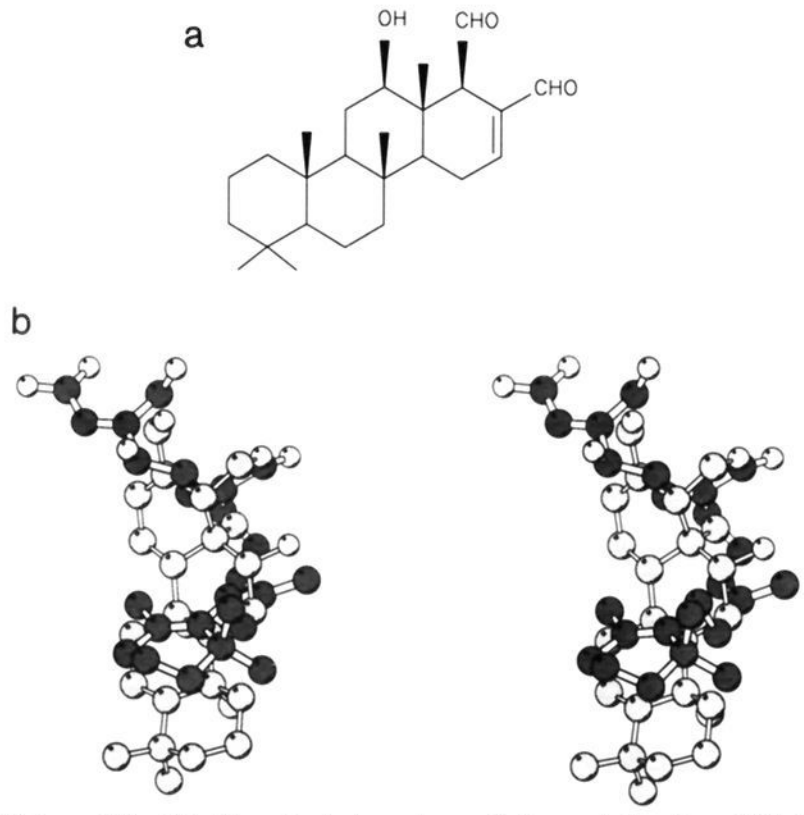

Figure 10. (a) Chemical structure of desacetylscalaradial (d-SCD). (b) Stereo representation[44] of the ASP-optimized superimposition of MLD (darker balls, thicker spokes) and d-SCD. Oxygen atoms are lighter and have a smaller radius than carbons. Hydrogen atoms have been omitted for clarity. The orientation of MLD is rougly similar to that in Figure 6.

modifies more than one lysine residue in the enzyme and implies that the MLD binding site can be different in other members of the PLA_2 superfamily. This idea is supported by the differences in reactivity observed among the different PLA_2s studied[3] and the complex kinetics of the reaction.[4,7]

By using the lower energy conformers and the GRID maps, 18 complexes other than those involving the active site of the enzyme were modeled by matching the corresponding interaction maps and the chemical structures of both ligand and receptor. On the basis of the results from the energy calculations on these complexes and the experimental evidence, a putative active conformation of MLD and a main putative MLD binding site in bv-PLA_2 were recognized. The proposed active conformation of the open form of MLD in bv-PLA_2 is a folded structure with a gauche$^+$ pseudodihedral angle. It is useful to compare this structure with that of desacetylscalaradial (d-SCD, Figure 10a), another irreversible inhibitor of bv-PLA_2 with a potency analogous to that of MLD,[22] in a low-energy conformation. d-SCD presents a 1,4-dialdehyde functionality, similar to that in MLD, and the initial reaction with bv-PLA_2 also entails the formation of a Schiff base.[11] The experimental evidence points to a common mechanism of action for MLD and d-SCD and is suggestive of common pharmacophoric groups in both structures. Figure 10b shows that in fact the aldehyde groups of both structures are nearly superimposed and that their hydrophobic regions are of similar size and shape (optimized similarity index for the molecular electrostatic potential = 0.57), which lends further credence to a common binding site and to the reported mechanism. The details of the interaction between bv-PLA_2 and d-SCD will be published elsewhere.

The putative major binding site for MLD is located on the surface of the enzyme, near the proposed interfacial binding surface[23] involved in the binding of PLA_2s to aggregated substrates. This site consists of two parts: a large hydrophobic pocket and a cationic site placed in such a way that only gauche$^+$ folded conformations of MLD can fit into it. The hydrophobic cavity is made up by residues 127–130 from a β-sheet and residues 101–105 and 113–116 from the antiparallel β-sheet, that is, the C-terminal portion of the enzyme. This result is in accord with experimental reports[6] that locate the major MLD binding site in the C-terminal region. The interaction in this hydrophobic pocket is not very specific and is governed primarily by hydrophobic forces. This is also in agreement with structure–activity studies,[10] which indicate that changes in the apolar region of the molecule do not affect the potency provided the hydrophobicity is conserved. It is noteworthy that introduction of a hydroxyl group in C-43 was found to produce a 15-fold decrease in potency. If the hydroxyl derivative is model-built from MLD in its complex with bv-PLA_2, it can be seen that the OH group would interact with Leu-50 and with the hydrocarbon part of Gln-127. The cationic site, on the other hand, is made up of Lys-94 and Arg-58 and interacts with the polar region of MLD by means of electrostatic forces between Arg-58 and mainly the carboxyl group of MLD. From the analysis of the interaction energy of the complex (Table III), we conclude that the initial fixation of MLD onto bv-PLA_2 is driven by the concerted binding of its apolar region (by means of hydrophobic forces) and its opened γ-lactone (by means of electrostatic interactions). This conclusion is in full agreement with the structure–activity relationships.[10]

Molecular orbital calculations suggest that the initial covalent modification of bv-PLA_2 by MLD could be achieved by means of a nucleophilic addition of Lys-94 to C-7 of MLD, leading to the formation of a Schiff base. It is remarkable that Lys-94 is the one residue mainly modified by MLD, according to an experimental report,[6] and that recent studies[11] have shown that the initial reaction between MLD and bv-PLA_2 is actually formation of an imine presumably involving the γ-lactone ring. All in all, our modeled complex allows us to explain some apparently contradictory experimental results: models based on reactivity with peptide sequences suggest a 2:1 lysine to MLD stoichiometry[6b] whereas studies based on incorporation of MLD analogues demonstrate a stoichiometry of incorporation of 1:1.[8] The present molecular model suggests that only one lysine does attack MLD, but also that one additional positive charge in the enzyme is required in order to interact with the carboxyl group, and that this interaction is important for the inhibitor to be potent. On the other hand, previous studies[7–9] with MLD analogues have indicated that irreversible inactivation of PLA_2 requires the presence of both the lactone ring and the unsaturated aldehyde portion of the hemiacetal ring and that irreversibility is mainly linked to the hemiacetalic ring. The chemical mechanism thus seems to entail reactions with the two aldehyde functionalities available in the open form of MLD. As no other nucleophilic group exists in the MLD binding site, we propose that irreversibility is achieved by secondary rearrangements in the covalent complex involving the imine and the second α,β-unsaturated aldehyde. Both aldehyde groups are roughly on the same plane in the putative active conformation of MLD, and the distance of 4.0 Å between their carbonyl carbon atoms implies that secondary reactions after the formation of the imine derivative should be possible. Work is in progress aimed at elucidating this second part of the mechanism of bv-PLA_2 inactivation by MLD.

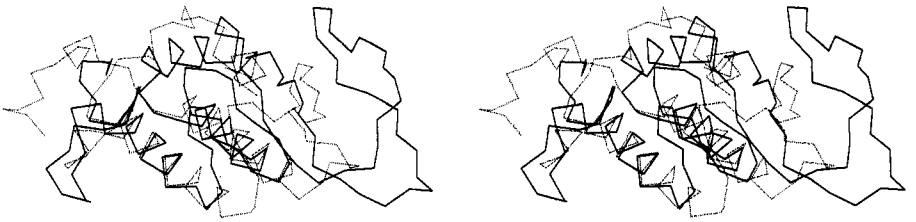

Figure 11. Three dimensional alignment of Cα atoms of bv-PLA_2 (solid lines) and *Naja naja atra* cobra venom PLA_2 (dotted lines).

The fact that MLD binds to a site apart from the active site in bv-PLA_2 poses the crucial question about the mechanism of inhibition, that is, how bv-PLA_2 is inhibited by MLD if the active site remains unaltered. It was shown above by molecular dynamics that MLD does not disrupt the protein environment in the surroundings of the binding site. As a matter of fact, the modified enzyme still presents a functional active site,[7,9] and by using manoalogue it has been demonstrated that inhibition is not due to a decrease in the fraction of enzyme bound to the interface.[7b] Since the major MLD binding site we now describe is located in the vicinity of the interfacial binding surface,[23] it can be postulated that MLD interferes with the "interfacial activation" of the enzyme. This mechanism is in fact suggested by some experimental findings,[6] although it is not clear how this interference is achieved. A tentative explanation can be put forth by comparing bv-PLA_2 and cobra venom PLA_2s: the MLD binding site in bv-PLA_2 is geometrically related to a recently proposed[24] phosphocoline binding site in cobra venom PLA_2s presumably involved in the activation of the enzyme. Both sites are in the same orientation with respect to the hydrophobic channel and the proposed interfacial binding surface (Figure 11). Moreover, both sites are structurally similar, presenting a cluster of aromatic rings, with capacity to give rise to π-cation interactions,[25] flanked by a lysine and a negatively charged residue. Therefore, the proposed MLD binding site may overlap with a phosphocoline binding site in the normal catalytic mechanism of the enzyme. Occupancy of this site by MLD, manoalogue, or d-SCD may block one of the anchoring points of the enzyme to the aggregated substrate in such a way that desolvation of the interface is not achieved and the enzyme cannot dislodge the substrate from the bilayer. Thus, MLD, manoalogue, or d-SCD can be thought of as competitive inhibitors of this anchoring phospholipid in bv-PLA_2. This hypothesis gains some support from the experimental finding that in the presence of excess phosphatidylcholine inactivation by SCD is reduced,[22] indeed pointing to a competitive mechanism. In this respect, the motion of the antiparallel β-sheet observed in the MLD–bv-PLA_2 simulation may recall a motion of activation of the enzyme when the phospholipid is bound in this site, allowing desolvation of the interface to take place. Such a displacement of part of the interfacial binding surface ("hydrophobic flap") is emerging as an activation mechanism in lipases.[26] One consequence of this mechanism is that modification of Lys-94 is not important in itself; its importance lies in the fact that it allows MLD to stay in its binding site.

A 40-fold difference in sensitivity to MLD has been found between bv-PLA_2 and cobra venom PLA_2s, whereas this factor is 250 when bv-PLA_2 and pancreatic PLA_2s are compared.[3] The high sensitivity of bv-PLA_2 can be understood if the structures of the different enzymes are overlaid (Figure 11). The structural comparison reveals that the major distinction between bv-PLA_2 and the class I/II PLA_2 superfamily is precisely the MLD binding site since it consists of a C-terminal extension of residues which is absent in the class I/II PLA_2s. Consequently, this optimal binding site does not exist in these enzymes. From this it can be inferred that the mechanism of inhibition by MLD may be different in the different PLA_2s, and that bv-PLA_2 is not a good model system on which to design and test novel antiinflammatory MLD-like compounds directed against proinflammatory PLA_2s.

Conclusions

Molecular modeling studies have identified a main putative binding site for MLD in bv-PLA_2, as well as a putative active conformation for the open form of MLD acting on this enzyme. This binding site is made up of a nonhomologous C-terminal extension of the protein sequence which is part of the interfacial binding surface of the enzyme, in accord with early experimental evidence.[6] It consists of two parts: a hydrophobic pocket corresponding to the C-terminal β-sheet (residues 127–130) and the antiparallel β-sheet (residues 101–105 and 113–116) and a cationic site comprising Arg-58 and Lys-94. The binding affinity of MLD in its open form, and hence its potency, stems from hydrophobic interactions arising from the apolar part of the molecule and electrostatic interactions between its carboxyl group and Arg-58. On the other hand, the efficacy (irreversibility) of MLD can be provided by the two aldehydes unmasked in its open form: the initial covalent addition is proposed to take place on the aldehyde formed upon opening of the γ-lactone ring, yielding an imine derivative with Lys-94. Moreover, the proximity of both aldehydes in this putative active conformation (C-7–C-20 distance = 4.0 Å) suggests that additional rearrangements with the opened hemiacetalic ring should be possible.

bv-PLA_2 inhibition appears to be due to occupation by MLD of a site overlapping a phosphocholine binding site in bv-PLA_2 presumably involved in the interface desolvation process. This binding site is absent in class I/II PLA_2s, which implies that bv-PLA_2 is not a good model system for developing MLD-like antiinflammatory compounds.

We are aware of the limitations of our computational approach. The docking procedure based on the GRID map complementarities is not completely free of user bias, and the energy-minimization protocol used for calculating the interaction of the different MLD conformers with each of the three sites explored did not allow for conformational flexibility of the enzyme and did not solve the "local minimum problem". Above all, the calculated binding energies are far from representing the actual binding free energy of MLD to the enzyme. Nevertheless, we feel that this contribution can represent an important step toward a better understanding of the mechanism of PLA_2 inactivation by MLD and MLD-like compounds. At worst,

Table IV. Additional AMBER Force-Field Parameters Used in the Study of MLD and Its Complex with bv-PLA$_2$

Bond Parameters $V_b = k_r(r - r_{eq})^2$

bond	k_r (kcal mol^{-1} Å^{-2})	r_{eq} (Å)	method
CS–C	377.	1.466	*a*
CS–CM	668.	1.337	*b*
CS–CS	555.	1.346	*a*
CS–CT	345.	1.488	*c*
C–HC	315.	1.090	*c*

Angle Parameters $V_\theta = k_\theta(\theta - \theta_{eq})^2$

angle	k_θ (kcal mol^{-1} radian^{-2})	θ_{eq} (deg)	method
O–C–HC	54.	121.0	*c*
CS–C–O	40.	120.0	*c*
CS–C–HC	23.	119.0	*c*
O2–C–CM	40.	120.0	*c*
C–CS–CT	60.	120.0	*c*
CM–CS–C	85.	128.2	*b*
CM–CS–CT	70.	119.7	analogy with CM–CM–CT
CS–CT–CT	60.	120.0	*c*
CS–CT–OH	80.	109.47	*c*
CS–CT–HC	40.	109.47	*c*
CT–CT–CS	45.	100.0	analogy with CT–CT–CM
CT–CS–CT	60.	120.0	*c*
CT–CS–CS	60.	120.0	*c*
C–CM–CS	85.	120.7	analogy with C–CM–CM
HC–CM–CS	35.	113.2	*b*
CT–CS–HC	40.	120.0	analogy with CT–CM–HC
CT–CM–CS	70.	119.7	analogy with CT–CM–CM

Torsion Angle Parameters $V_\phi = (V_\eta/2)[1 + \cos(\eta\Phi - \gamma)]$

angle	NTOR	$V_\eta/2$ (kcal mol^{-1})	γ	η	method
X–CS–CS–X	4	25.3	180.0	2.0	*a*
X–CS–CM–X	4	24.4	180.0	2.0	*b*
X–CS–OH–X	2	1.8	0.0	2.0	*a*
X–CS–CT–X	6	0.5	0.0	3.0	*a*
X–C–CS–X	4	2.7	180.0	2.0	*a*

Improper Torsion Angle Parameters

angle	$V_\eta/2$ (kcal mol^{-1})	γ	η	method
C–CM–HC–CS	14.0	180.0	2.0	analogy
CT–CS–CS–CT	10.5	180.0	2.0	analogy
CT–CT–CS–CT	10.5	180.0	2.0	analogy
CM–CT–CS–CT	10.5	180.0	2.0	analogy
CT–CM–CS–HC	10.5	180.0	2.0	analogy
CM–CT–CS–C	10.5	180.0	2.0	analogy
CS–O–C–HC	1.0	180.0	2.0	analogy

[a] Interpolation, as explained in ref 29. [b] Alagona et al. *J. Comput. Chem.* 1991, *12*, 934–942. [c] Extrapolation from CHARMM parameters (Brooks, B. R.; et al. *J. Comput. Chem.* 1983, *4*, 187–217).

our results may help to provide new ground for experimental verification.

Methodology

All of the programs described below were implemented on a Control Data CYBER 910B-537, a CYBER 910–480, and a Silicon Graphics INDIGO workstations.

(a) Parameter Assignment. The open and extended form of MLD (Figure 1b) was built with standard bond lengths and angles by using the molecular modeling package INSIGHT-II.[27] The molecular mechanics and molecular dynamics calculations were performed with the AMBER 3.0 suite of programs.[28] The all-atom AMBER force field[29] was employed throughout with one exception noted below. Some additional bonded parameters were needed, and these can be found in Table IV, along with the derivation procedure. One new atom type was introduced (CS),

Table V. MEP-Derived Point Charges and AMBER Atom Types for MLD

atom	atom type	charge	atom	atom type	charge
O1	O2	–0.7404	H33	HC	0.1239
C2	C	0.7844	H34	HC	0.1404
O3	O2	–0.7686	H35	HC	0.1611
C4	CM	–0.2090	C36	CT	–0.4475
H5	HC	0.0939	H37	HC	0.1599
C6	CS	–0.3728	H38	HC	0.1595
C7	C	0.6078	C39	CT	–0.2709
O8	O	–0.6388	H40	HC	0.1659
H9	HC	0.0719	H41	HC	0.1004
C10	CT	0.6793	C42	CS	–0.1760
O11	OH	–0.6858	C43	CS	0.0634
H12	HO	0.3902	C44	CT	–0.2305
H13	HC	–0.0112	H45	HC	0.0932
C14	CT	–0.5887	H46	HC	0.1285
H15	HC	0.2261	H47	HC	0.0661
H16	HC	0.1544	C48	CT	–0.1935
C17	CM	–0.0877	H49	HC	0.1002
H18	HC	0.1422	H50	HC	0.0703
C19	CS	0.0208	C51	CT	–0.0654
C20	C	0.3626	H52	HC	0.0376
O21	O	–0.4338	H53	HC	0.0324
H22	HC	0.0303	C54	CT	–0.1147
C23	CT	–0.3237	H55	HC	0.0232
H24	HC	0.1085	H56	HC	0.0321
H25	HC	0.1026	C57	CT	0.3889
C26	CT	0.1356	C58	CT	–0.3543
H27	HC	0.0251	H59	HC	0.0897
H28	HC	0.0232	H60	HC	0.0656
C29	CM	–0.3366	H61	HC	0.0985
H30	HC	0.1462	C62	CT	–0.2941
C31	CS	0.2388	H63	HC	0.0476
C32	CT	–0.5020	H64	HC	0.0877
			H65	HC	0.0661

defined as a nonaromatic sp^2 carbon singly bonded to two other carbon atoms, for which the van der Waals parameters of the AMBER C atom type were taken. In order to include the electrostatic energy term for MLD, atom-centered charges were calculated[30] so as to reproduce on a surface beyond the van der Waals surface the quantum mechanical molecular electrostatic potential (MEP) generated by using the semiempirical molecular orbital AM1[31] method as implemented in the MOPAC[32] program. These charges were used in the conformational search procedure. As MEP-derived charges are slightly dependent on molecular conformation,[33] new charges (Table V) were assigned when the proposed active conformation of MLD was selected upon completion of the conformational search and docking procedure (*vide infra*), using the same method as before.

(b) Conformational Search. The phase space for MLD was sampled by using the following quenched molecular dynamics protocol (Chart I): An infinite cutoff for the nonbonded interactions and a continuum aqueous solvent with a dielectric constant $\epsilon = 4r_{ij}$ was employed during the whole procedure. The extended conformation of MLD was energy minimized by using 25 steps of the steepest descent method and then switching over to the conjugate gradient method until the root-mean-square gradient was less than 0.01 kcal mol^{-1} Å^{-1}. A conformational search began at this point using classical molecular dynamics by heating the molecule from 2 K to 1000 ± 10 K in 5 ps using velocity scaling, with the initial velocities reassigned from a Maxwell–Boltzmann distribution at each new temperature. After a further 5 ps of equilibration, a 100-ps trajectory was simulated and coordinates were saved with a time resolution of 0.1 ps. All bonds involving hydrogens were constrained to their equilibrium values by means of the SHAKE algorithm[34] which allowed a time step of 0.002 ps to be employed. One hundred conformations separated by 1 ps were then selected, and each one of them was subjected to extensive steepest descent energy minimization until the root-mean-square gradient was less than 0.01 kcal mol^{-1} Å^{-1}. The 10 lower potential energy structures, along with other 20 structures obtained by extracting one set of coordinates every 5 ps from the trajectory, were simulated at 300 ± 10 K during 10 ps each. The 15 resulting structures having a potential energy below 25 kcal mol^{-1}, taking both simulations together, were finally

subjected to energy minimization as before and were also optimized in MOPAC using the AM1 Hamiltonian. The final set converged to nine distinct minimum energy conformers.

(c) Analysis of the Conformational Search. Additional programs were required for analyzing the data from the simulations and they were developed in Fortran-77 by A.R.O.

A simple analysis in the cartesian space of the conformations surveyed by the simulation involves computing the root-mean-square differences between all pairs of coordinates obtained by periodically sampling the trajectory. In this way, a displacement autocorrelation matrix (DAM) and a displacement autocorrelation function (DAF) can be defined as follows:

$$DAM\ (t, t+\Delta t) = \left[\frac{\sum_i (x_i(t) - x_i(t+\Delta t))^2}{n}\right]^{1/2} \quad (1)$$

$$DAF\ (\tau) = \left\langle \left[\frac{1}{n}\sum_{i=1}^{i=n} (x_i(t+\tau) - x_i(t))^2\right]^{1/2} \right\rangle_t \quad (2)$$

In both equations, i varies over the x, y, and z coordinates of all the atoms of the molecule, n is the number of atoms in the molecule, t is simulation time, τ is a displacement time, and $\langle\ \rangle_t$ represents an average over t.

Another way to analyze the conformational space sampled in the simulation is to examine the torsion angles. Each torsion angle involving single bonds was divided into three 120° intervals (−, 0, +) so as to divide the dihedral space into many small hypercubes.[14] For each of the 1000 coordinate sets saved along the dynamics trajectory each of the torsions defined (τ_1–τ_9) was assigned to one of the hypercubes, and the number of different conformational hypercubes found was counted.

(d) Docking Procedure. Both ligand and receptor were systematically explored in search of mutually complementary binding sites, making use of the GRID[16] suite of programs.[35] For MLD, the exploration was carried out on each of the nine lower potential energy conformers found after the conformational search; these were taken to be potential candidates for the molecule in its active conformation. For the receptor, the structure of bv-PLA_2 complexed with a transition-state analogue crystallographically determined at 2.0-Å resolution ($R = 0.198$)[12] was employed. The receptor coordinates were prepared in several stages: (i) the substrate analogue was deleted and all the hydrogen atoms were added to the enzyme and to the 67 crystallographically determined water molecules by using standard bond lengths and angles;[27] (ii) the hydrogen atoms were reoriented and optimized by using conjugate gradient energy minimization (8.0-Å cutoff) while keeping the heavy atoms frozen; (iii) the energy of the whole system was relaxed by using 1500 steps of conjugate gradient energy minimization (8.0-Å cutoff, update of pairs list every 50 steps for nonbonded interactions, and a dielectric constant $\epsilon = 4r_{ij}$), while the heavy atoms of the enzyme were constrained to their crystallographic positions by using a harmonic potential with a force constant of 100 kcal mol^{-1} $Å^{-2}$ (during this procedure, the van der Waals energy of the system dropped considerably, but the enzyme coordinates were essentially the same as those found in the crystal structure); (iv) all the water molecules and hydrogens in the minimized structure were removed, but the calcium ion in the active site was preserved and assigned a charge of +2.

The interactions of methyl and multiatom carboxyl probes with the protein, and of methyl and charged sp^3 amino probes with the nine MLD conformers were calculated at a lattice of points established throughout and around the molecules,[16] contoured at appropriate energy levels and displayed by computer graphics.[27] The dielectric constants chosen were 4.0 for the macromolecule and 80.0 for the bulk water. All searches were carried out using a 55 × 45 × 40 Å box around the macromolecule and a clearance of 5 Å around the ligands, with the grid points spaced at 0.5 Å in both cases. Only pockets on the receptor surface large enough to lodge the ligand were analyzed, as well as the active site, which was used as a negative control. As a result, two putative binding sites for MLD in bv-PLA_2 were identified. Each of the nine lower energy conformers of MLD were then manually docked into each of these three sites on the basis of the complementarity between the respective GRID maps and the chemical structures. A total of 27 complexes were thus generated, which were optimized in AMBER by using 250 steps of steepest descent energy minimization (8-Å cutoff, $\epsilon = 4r_{ij}$). For ease of comparison and to speed up the calculations, the coordinates of the enzyme were kept fixed at their crystallographic positions. The differential binding energy for MLD in each of these complexes (ΔBE) was then calculated as follows:

$$\Delta BE = \Delta E_i + \Delta\Delta E_d + \Delta\Delta E_e + \Delta SFE_b \quad (3)$$

where ΔE_i is the relative interaction energy between each MLD conformer and the enzyme as calculated with the ANAL module in AMBER, $\Delta\Delta E_d$ is the relative variation in conformational energy of each MLD conformer calculated using the semiempirical AM1 hamiltonian within MOPAC, $\Delta\Delta E_e$ is the relative conformational energy change of the enzyme (which is 0 in this case), and ΔSFE_b is the relative change in solvation free energy for each complex. The SFE is an empirical correction accounting for the contribution of solvation to the free energy of binding of small molecules to proteins, calculated by program FRENS[19] according to the following equation:

$$SFE_{binding} = SFE_{complex} - (SFE_{enzyme} + SFE_{drug}) \quad (4)$$

(e) Molecular Dynamics Simulations. Once the putative active conformation of MLD and the main putative binding site in bv-PLA_2 were unravelled, a molecular dynamics study of the complex was undertaken. All hydrogens were explicitly represented in MLD whereas nonpolar hydrogens of bv-PLA_2 were treated by way of the united-atom[36] approach for computational efficiency, except for those belonging to residues making up the MLD binding site (see Results and Discussion), which were also modeled as all-atom.[29] The energy of the complex was relaxed, using a cutoff of 8.0 Å and a distance-dependent dielectric constant ($\epsilon = 4r_{ij}$) in two steps: first, only the ligand was allowed to move, and then the whole complex was energy minimized. Only small distorsions in the polar extreme of MLD were observed, which enhanced its interaction with Arg-58. This final coordinate set was used as input for the subsequent molecular dynamics simulation. In order to include the effects of solvation explicitly, a spherical "cap" of 469 TIP3P water molecules,[37] generated from a Monte Carlo simulation, was added to the complex within 15 Å of the center of mass of the main putative MLD binding site. A harmonic radial potential with a force constant of 0.6 kcal mol^{-1} $Å^{-2}$ restrained any water from leaving this 15-Å boundary.[38] In the solvation process, any water molecule with its oxygen atom closer than 2.8 Å to any atom of the complex or with any hydrogen atom closer than 1.5 Å to any atom of the complex was eliminated. The water molecules, MLD, and protein residues containing any atom within this water sphere (residues 101–119, 127–130, 115, 94, 58) were allowed to move whereas the residues without were fixed at their starting locations although they were included in the determination of the forces. The resulting system was then optimized by using 500 steps of steepest descent energy minimization followed by conjugate gradient until the root-mean-square value of the potential energy gradient was below 0.01 kcal mol^{-1} $Å^{-1}$. In a 3-ps heating phase, the temperature was raised from 0.2 to 300 K in steps of 20 K over 0.2-ps blocks, the velocities being reassigned according to a Maxwell–Boltzmann distribution at each new temperature. The system was further equilibrated for 10 ps. A 100-ps trajectory was then simulated, and coordinates were saved every 0.1 ps. All bonds involving hydrogens were constrained to their equilibrium values using the SHAKE algorithm,[34] a time step of 0.002 ps was employed, and the nonbonded pairs list was updated every 25 steps. The temperature was maintained at 300 K by coupling to an external heating bath.[39] A cutoff of 8.0 Å was used for the nonbonded interactions and a dielectric constant $\epsilon = r_{ij}$ was employed even though water molecules were present. Given that the putative MLD binding site is on the surface of the protein, and that a "cap" of water molecules was used, the full dielectric effect of the solvent will not be present; instead a macroscopic dielectric constant is warranted.[40] The effect of this dielectric constant was tested by

running two independent simulations of 50 ps each on the X-ray bv-PLA_2 structure, under the solvation conditions described above, and utilizing either $\epsilon = 1$ or $\epsilon = r_{ij}$. The last 20 ps of each simulation were averaged, and the two resulting structures were energy relaxed and compared with the X-ray structure. When $\epsilon = 1$, distortions were observed in the loop region 101–119 (root-mean-square displacement = 2.95 Å) and in several side chains, particularly Glu-110 and Glu-107 (electrostatic repulsion). On the contrary, when $\epsilon = r_{ij}$ the structure remained very close to the crystallographic structure (root-mean-square displacement of the same region = 0.90 Å).

(f) Molecular Orbital Calculations. The minimized average structure of MLD in its complex with bv-PLA_2 (see under Results) was optimized by means of the AM1 hamiltonian within MOPAC to a gradient norm of less than 0.01 kcal mol^{-1} $Å^{-1}$ (or kcal mol^{-1} rad^{-1}). The DENSITY program[41] was then used for generating the maps of electron density distribution and molecular orbital intensity within the MLD molecule. The three-dimensional structures, and the frontier orbital and electron density extensions were visualized in INSIGHT and helped in the interpretation of the quantitative results.

(g) Superposition of MLD and d-SCD. The ASP (automated similarity package) program[42] was employed to superimpose the structure of d-SCD upon the docked conformation of MLD and to evaluate the molecular similarity index. The shape of the charge distribution of two superimposed molecules, a and b, may be compared using an index (R_{ab}) defined by Carbó et al.:[43]

$$R_{ab} = \frac{\int \rho_A \rho_B d\upsilon}{(\int \rho_A^2 d\upsilon)^{1/2} (\int \rho_B^2 d\upsilon)^{1/2}} \quad (5)$$

where ρ_a and ρ_b are the electron densities of molecules a and b, respectively. The numerator is a measure of the overlap of charge density for the two superimposed molecules, and the denominator is a normalization factor. ASP uses this same reasoning but compares the molecules in terms of their electrostatic potentials which are computed from atom-centered point partial charges on a three-dimensional grid surrounding the two molecules. Calculated indices range from +1.0 (perfect similarity) to −1.0.

MOPAC-optimized geometries and MEP-derived charges were used for both MLD and d-SCD. The carboxylate tail of MLD was excluded from the similarity calculations since the highly negative electrostatic potential around this part of the molecule would have masked more subtle differences in other regions. ASP was used to optimize the superimposition by allowing d-SCD to rotate and translate in space with respect to MLD until the relative orientation of both molecules provided the best similarity index.

Supplementary Material: Coordinates of the noncovalent MLD–bv-PLA_2 complex in PDB format are available from the authors on request (e-mail:ffgago@alcala.es).

Acknowledgment. We thank Professor Paul B. Sigler for kindly providing us with the coordinates of *Naja naja atra* and bee venom PLA_2s, Dr. David Eisenberg for his program for calculating solvation free energies, Dr. Chris Reynolds for his program to compute point charges, Oxford Molecular Ltd. for the program ASP, and Biosym Technologies, Inc., for a license to use their graphics programs. We are also grateful to Dr. Selma Arias and Dr. Henry Rzepa for helpful comments on nucleophilicity. This research has been financed in part by Laboratorios Menarini, S. A. (Badalona, Spain), Comisión Interministerial de Ciencia y Tecnología (CICYT), and the University of Alcalá de Henares (Madrid, Spain).

References

(1) de Silva, E. D.; Scheuer, P. J. Manoalide, an antibiotic sesterterpenoid from the marine sponge *Luffariella variabilis*. *Tetrahedron Lett.* **1980**, *21*, 1611–1614.
(2) (a) de Freitas, J. C.; Blankmeier, L. A.; Jacobs, R. S. In vitro inactivation of the neurotoxic action of β-bungarotoxin by the natural product Manoalide. *Experientia* **1984**, *40*, 864–865. (b) Lombardo, D.; Dennis E. A. Cobra Venom Phospholipase A_2 Inhibition by Manoalide. *J. Biol. Chem.* **1985**, *260*, 7234–7240. (c) Jacobs, R. S.; Culver, P. B.; Langdon, R. B.; O'Brien, T.; White, S. J. Some pharmacological observations on marine natural products. *Tetrahedron* **1985**, *41*, 981–984.
(3) Bennett, C. F.; Mong, S.; Clarke, M. A.; Kruse, L. I.; Crooke, S. T. Differential effects of manoalide on secreted and intracellular phospholipases. *Biochem. Pharmacol.* **1987**, *36*, 733–740.
(4) Glaser, K. B.; Jacobs, R. S. Molecular pharmacology of manoalide: inactivation of bee venom phospholipase A_2. *Biochem. Pharmacol.* **1986**, *35*, 449–453.
(5) Mann, J. Sponges to wipe away pain. *Nature* **1992**, *358*, 540.
(6) (a) Glaser, K. B.; Vedvick, T. S.; Jacobs, R. S. Inactivation of phospholipase A_2 by manoalide: localization of the manoalide binding site on bee venom phospholipase A_2. *Biochem. Pharmacol.* **1988**, *37*, 3639–46. (b) Glaser, K. B.; Jacobs, R. S. Inactivation of bee venom phospholipase A_2 by manoalide: a model based on the reactivity of manoalide with amino acids and peptide sequences. *Biochem. Pharmacol.* **1987**, *36*, 2079–2086.
(7) (a) Reynolds, L. J.; Morgan, B. P.; Hite, G. A.; Mihelich, E. D.; Dennis, E. A. Phospholipase A_2 inhibition and modification by manoalogue. *J. Am. Chem. Soc.* **1988**, *110*, 5172–5177. (b) Ghomashchi, F.; Yu, B.-Z.; Mihelich, E. D.; Jain, M. K.; Gelb, M. H. Kinetic characterization of phospholipase A_2 modified by manoalogue. *Biochemistry* **1991**, *30*, 9559–9569.
(8) Reynolds, L. J.; Mihelich, E. D.; Dennis, E. A. Inhibition of venom phospholipases A_2 by manoalide and manoalogue: stoichiometry of incorporation. *J. Biol. Chem.* **1991**, *266*, 16512–16517.
(9) Deems, R. A.; Lombardo, D.; Morgan, B. P.; Mihelich, E. D.; Dennis, E. A. The inhibition of phospholipase A_2 by manoalide and manoalide analogues. *Biochim. Biophys. Acta* **1987**, *917*, 258–268.
(10) Glaser, K. B.; de Carvalho, M. S.; Jacobs, R. S.; Kernan, M. R.; Faulkner, D. J. Manoalide: structure-activity studies and definition of the pharmacophore for phospholipase A_2 inactivation. *Mol. Pharmacol.* **1989**, *36*, 782–788.
(11) Potts, B. C. M.; Faulkner D. J.; de Carvalho M. S.; Jacobs, R. S. Chemical mechanism of inactivation of bee venom phospholipase A_2 by the marine natural products manoalide, luffariellolide, and scalaradial. *J. Am. Chem. Soc.* **1992**, *114*, 5093–5100.
(12) Scott, D. L.; Otwinowski, Z.; Gelb, M. H.; Sigler, P. B. Crystal structure of bee-venom phospholipase A_2 in a complex with a transition-state analogue. *Science* **1990**, *250*, 1563–1566.
(13) Part of this work has been presented as an oral communication: Ortiz, A. R.; Pisabarro, M. T.; Gago, F. Molecular Mechanism of Phospholipase A_2 Inhibition by Manoalide. XIIth International Symposium on Medicinal Chemistry: Basel, 1992.
(14) Bruccoleri, R. E.; Karplus, M. Conformational Sampling Using High-Temperature Molecular Dynamics. *Biopolymers* **1990**, *29*, 1847–1862.
(15) Mackay, D. H. J.; Cross, A. J.; Hagler, A. T. The Role of Energy Minimization in Simulation Strategies of Biomolecular Systems. In *Prediction of Protein Structure and the Principles of Protein Conformation*; Fasman, G. D., Ed.; Plenum Press: New York, 1989; pp 317–358.
(16) (a) Goodford, P. J. A Computational Procedure for Determining Energetically Favorable Binding Sites on Biologically Important Macromolecules. *J. Med. Chem.* **1985**, *28*, 849–857. (b) Boobyer, D. N.; Goodford, P. J.; Mc Whinnie, P. M.; Wade, R. C. New hydrogen-bond potentials for use in determining energetically favorable binding sites on molecules of known structure. *J. Med. Chem.* **1989**, *32*, 1083–1094.
(17) Ortiz, A. R.; Orozco, M.; Luque, F. J.; Pisabarro, M. T.; Gago, F. Unpublished results.
(18) Lee, B.; Richards, F. M. The Interpretation of Protein Structure: Estimation of Static Accessibility. *J. Mol. Biol.* **1971**, *55*, 379–400.
(19) Eisenberg, D.; McLachlan, A. D. Solvation Energy in Protein Folding and Binding. *Nature* **1986**, *319*, 199–203.
(20) Chao, T.-M.; Baker, J.; Hehre, W. J.; Kahn, S. D. Models for Selectivity in Organic Reactions. *Pure Appl. Chem.* **1991**, *63*, 283–288 and references cited herein.
(21) Menger, F. M. Nucleophilicity and Distance. In *Nucleophilicity*; Harris, J. M., McManus, S. P., Eds.; Advances in Chemistry Series 215; American Chemical Society: Washington, 1987 pp 209–218.
(22) de Carvalho, M. S.; Jacobs, R. S. Two-step inactivation of bee venom phospholipase A_2 by scalaradial. *Biochem. Pharmacol.* **1991**, *42*, 1621–1626.
(23) Scott, D. L.; White, S. P.; Otwinowski, Z.; Yuan, W.; Gelb, M. H.; Sigler, P. B. Interfacial catalysis: the mechanism of phospholipase A_2. *Science* **1990**, *250*, 1541–1546.
(24) Ortiz, A. R.; Pisabarro, M. T.; Gallego, J.; Gago, F. Implications of a consensus recognition site for phosphatidylcholine separate from the active site in cobra venom phospholipases A_2. *Biochemistry* **1992**, *31*, 2887–2896.
(25) Dougherty, D. A.; Stauffer, D. A. Acetylcholine Binding by a Synthetic Receptor: Implications for Biological Recognition. *Science* **1990**, *250*, 1558–1560.
(26) Blow, D. Lipases Reach the Surface. *Nature* **1991**, *351*, 444–445.

(27) INSIGHT-II (version 2.1.0) 1992. Biosym Technologies. 9685 Scranton Road, San Diego, CA 92121-2777.
(28) Seibel, G.; Singh, U. C.; Weiner, S. J.; Caldwell, J.; Kollman, P. A. *AMBER (UCSF): Assisted Model Building with Energy Refinement*, version 3.0, Revision A. Department of Pharmaceutical Chemistry, University of California: San Francisco, 1989.
(29) Weiner, S. J.; Kollman, P. A.; Nguyen, D. T.; Case, D. A. An All Atom Force Field for Simulations of Proteins and Nucleic Acids. *J. Comput. Chem.* **1986**, *7*, 230–252.
(30) Ferenczy, G. G.; Reynolds, C. A.; Richards, W. G. Semiempirical AM1 electrostatic potentials and AM1 electrostatic potential derived charges: A comparison with *ab initio* values. *J. Comput. Chem.* **1990**, *11*, 159–169.
(31) Dewar, M. J. S.; Zoebisch, E. G.; Healy, E. F.; Stewart, J. J. P. AM1: A New General Purpose Quantum Mechanical Molecular Model. *J. Am. Chem. Soc.* **1985**, *107*, 3902–3909.
(32) Stewart, J. J. P. MOPAC: A General Molecular Orbital Package, version 5.0; *QCPE 455*, Quantum Chemistry Program Exchange, Indiana University, Bloomington, IN 47405.
(33) (a) Schaumberger, M.; Köhler, J. Charge distributions of phosphorylcholine and its derivatives. *J. Comput. Chem.* **1992**, *13*, 318–328. (b) Reynolds, C. A.; Essex, J. W.; Richards, W. G. Atomic Charges for Variable Molecular Conformations. *J. Am. Chem. Soc.* **1992**, *114*, 9075–9079.
(34) Ryckaert, J. P.; Ciccotti, G.; Berendsen, H. J. C. Numerical Integration of the Cartesian Equations of Motion of a System with Constraints: Molecular Dynamics of n-alkanes. *J. Comp. Phys.* **1977**, *23*, 327–341.
(35) GRIN, GRID and GRAB, version 8.0, Molecular Discovery Ltd., 1991.
(36) Weiner, S. J.; Kollman, P. A.; Case, D. A.; Singh, U. C.; Ghio, C.; Alagona, C.; Profeta, S.; Weiner, P. A New Force Field for Molecular Mechanical Simulation of Nucleic Acids and Proteins. *J. Am. Chem. Soc.* **1984**, *106*, 765–784.
(37) Jorgensen, W. L.; Chandrasekhar, J.; Madura, J. D.; Impey, R. W.; Klein, M. L. Comparison of Simple Potential Functions for Simulating Liquid Water. *J. Chem. Phys.* **1983**, *79*, 926–935.
(38) Brooks, C. L.; Brünger, A.; Karplus, M. Active Site Dynamics in Protein Molecules: A Stochastic Boundary Molecular Dynamics Approach. *Biopolymers* **1985**, *24*, 843–865.
(39) Berendsen, H. J. C.; Postma, J. P. M.; van Gunsteren, W. F.; Di Nola, A.; Haak, J. R. Molecular Dynamics with Coupling to an External Bath. *J. Chem. Phys.* **1984**, *81*, 3684–3690.
(40) Daggett, V.; Schroder, S.; Kollman, P. Catalytic Pathway of Serin-proteases: Classical and Quantum Mechanical Calculations. *J. Am. Chem. Soc.* **1991**, *113*, 8926–8935.
(41) Stewart, J. J. P. DENSITY: A Package to Produce Density Plots from MOPAC Calculations. *QCPE 492*, Quantum Chemistry Program Exchange, Indiana University, Bloomington, IN 47405.
(42) Burt, C.; Huxley, P.; Richards, W. G. The Application of Molecular Similarity Calculations. *J. Comput. Chem.* **1990**, *11*, 1139–1146.
(43) Carbó, R.; Leyda, L.; Arnau, M. An Electron Density Measure of the Similarity Between Two Compounds. *Int. J. Quant. Chem.* **1980**, *17*, 1185–1189.
(44) Kraulis, P. J. Molscript: a Program to Produce both Detailed and Schematic Plots of Protein Structures. *J. Appl. Crystallogr.* **1991**, *24*, 946–950.